Astron. Astrophys. 364, L13–L18 (2000)

ASTRONOMY AND ASTROPHYSICS

LETTER

Letter to the Editor

VLT-detection of two edge-on Circumstellar Disks in the ρ Oph dark cloud*

W. Brandner[1], **S. Sheppard**[1], **H. Zinnecker**[2], **L. Close**[3], **F. Iwamuro**[4], **A. Krabbe**[5**], **T. Maihara**[4], **K. Motohara**[6], **D.L. Padgett**[7], **and A. Tokunaga**[1]

[1] University of Hawaii, Institute for Astronomy, 2680 Woodlawn Drive, Honolulu, HI 96822, USA (brandner@ifa.hawaii.edu, sheppard@ifa.hawaii.edu, tokunaga@ifa.hawaii.edu)
[2] Astrophysikalisches Institut Potsdam, An der Sternwarte 16, 14482 Potsdam, Germany (hzinnecker@aip.de)
[3] European Southern Observatory, Karl-Schwarzschild Strasse 2, 85748 Garching, Germany (lclose@eso.org)
[4] Kyoto University, Department of Physics, Kitashirakawa, Kyoto 606-8502, Japan (iwamuro@cr.scphys.kyoto-u.ac.jp, maihara@cr.scphys.kyoto-u.ac.jp
[5] Deutsches Zentrum für Luft- und Raumfahrt, Institut für Weltraumsensorik und Planetenerkundung, Rutherfordstrasse 2, 12489 Berlin, Germany (krabbe@dlr.de)
[6] Subaru Telescope, National Astronomical Observatory of Japan, 650 North A'ohoku Place, Hilo, HI 96720, USA (motohara@subaru.naoj.org)
[7] Jet Propulsion Laboratory, IPAC 100-22, California Institute of Technology, Pasadena, CA 91125, USA (dlp@ipac.caltech.edu)

Received 10 August 2000 / Accepted 7 September 2000

Abstract. Observations of the ρ Ophiuchi star forming region with VLT ANTU and ISAAC under $0.''35$ seeing conditions reveal two bipolar reflection nebulosities intersected by central dust lanes. The sources (OphE-MM3 and CRBR 2422.8−3423) can be identified as spatially resolved circumstellar disks viewed close to edge-on, similar to edge-on disk sources discovered previously in the Taurus and Orion star forming regions. Millimeter continuum fluxes yield disk masses of the order of 0.01 $M_\odot$, i.e. about the mass deemed necessary for the minimum solar nebula. Follow-up spectroscopic observations with SUBARU and CISCO show that both disk sources exhibit featureless continua in the K-band. No accretion or outflow signatures were detected. The slightly less edge-on orientation of the disk around CRBR 2422.8−3423 compared to HH 30 leads to a dramatic difference in the flux seen in the ISOCAM 4.5 μm to 12 μm bands. The observations confirm theoretical predictions on the effect of disk geometry and inclination angle on the spectral energy distribution of young stellar objects with circumstellar disks.

Key words: stars: circumstellar matter – stars: formation – stars: pre-main sequence – Galaxy: open clusters and associations: individual: rho Ophiuchi dark cloud

1. Introduction

One of the focal points of current astronomical research is the search for circumstellar disks and a study of their transformation into planetary systems. The aim is to understand how the solar system evolved, and to determine how many other planetary systems might exist in the Galaxy.

The huge brightness difference of typically 10^6 to 1 between the central star and light scattered from the disk surface (Sonnhalter et al. 1995; Boss & Yorke 1996) makes it challenging to detect and resolve circumstellar disks in the optical and near-infrared. If the disk, however, is seen close to edge-on, it acts as a natural coronagraph and blocks out the light from the central star. The typical signature for such an alignment is a bipolar reflection nebula intersected by a central dust lane (Whitney & Hartmann 1992; Sonnhalter et al. 1995; Burrows et al. 1996). Edge-on circumstellar disk sources have been discovered in the Orion nebula (McCaughrean & O'Dell 1996) and in the Taurus T association (e.g., Burrows et al. 1996, Lucas & Roche 1997, Padgett et al. 1999, Koresko 1998, Stapelfeldt et al. 1998, Monin & Bouvier 2000).

It has already become apparent that different environments affect the evolution of circumstellar disks in various ways. In dense regions with many hot, luminous early type stars like, e.g., the Trapezium cluster in Orion or the starburst cluster NGC 3603, the harsh radiation environment leads to a rapid photoevaporation of circumstellar disks (O'Dell et al. 1993; McCullough et al. 1995; Störzer & Hollenbach 1999; Brandner et al. 2000). The low-density Taurus T association, on the other hand, is a more benign environment. Because of the high multiplicity among T Tauri stars in Taurus (Ghez et al. 1993, Leinert et

* Based on observations at the European Southern Observatory, Paranal (ESO Prop ID 63.I-0691), the NAOJ SUBARU telescope at Mauna Kea, Hawai'i, the ESA Infrared Space Observatory, and the NASA/ESA Hubble Space Telescope obtained at the Space Telescope Science Institute, which is operated by the Association of Universities for Research in Astronomy, Inc., under the NASA contract NAS5-26555.

** new address: University of California at Berkeley, Department of Physics, 366 LeConte Hall #7300, Berkeley, CA 94720-7300, USA

Table 1. Coordinates and near infrared photometry (in the 2MASS photometric system) of the edge-on circumstellar disks.

Target	α(2000) [hms]	δ(2000) [$\circ$ $'$ $''$]	J [mag]	H [mag]	K [mag]	L[a] [mag]
OphE-MM3 (disk 1)	16 27 05.91	-24 37 08.2	...	18.4±0.2	15.4±0.2	...
CRBR 2422.8−3423 (disk 2)	16 27 24.61	-24 41 03.3	>21.0	18.0±0.2	13.3±0.1	9.7±0.1

[a] Comerón et al. 1993

al. 1993, Köhler & Leinert 1998), however, the majority of circumstellar disks might be affected by tidal truncation, like, e.g., HK Tau/c (Koresko 1998, Stapelfeldt et al. 1998) or HV Tau C (Monin & Bouvier 2000).

The ρ Ophiuchi molecular cloud complex is the formation site of a proto-open cluster with a gaseous mass of around 550 $M_\odot$ (Wilking & Lada 1983) and at least 100 stellar members (Comerón et al. 1993; Barsony et al. 1997; Kenyon et al. 1998). Its stellar density is intermediate between that of the Taurus T association and the Trapezium cluster. The absence of hot, luminous early-type stars ensures that circumstellar disks are not subject to photoevaporation. The ρ Oph region appears to be a more typical representative of the dominant star formation mode in the Galaxy than the low density environment of the wide-spread Taurus T association with its high percentage of binary and multiple systems.

In an effort to identify spatially resolved circumstellar disks in various environments, we carried out a VLT/ISAAC survey of southern starforming regions (Zinnecker et al. 1999). The survey also aimed at establishing a sample of circumstellar disk sources which are suitable for detailed follow-up studies with the VLT-Interferometer and the Atacama Large Millimeter Array.

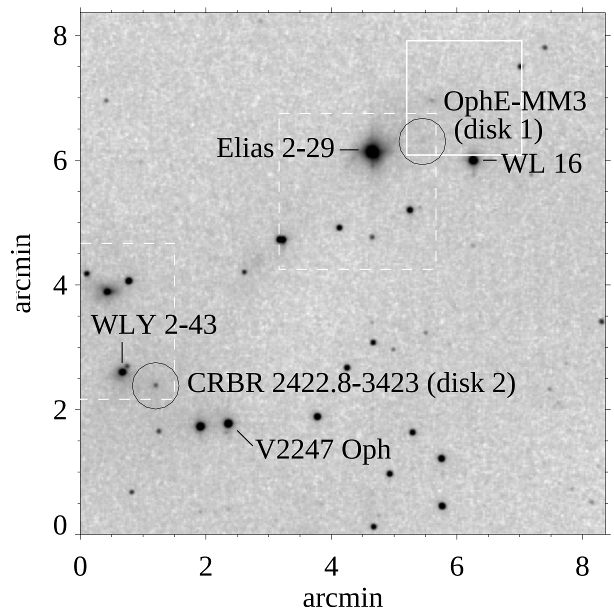

Fig. 1. K-band finding chart based on 2MASS atlas images. The dashed lines indicate the area covered by the two VLT/ISAAC pointings, and the solid lines mark the area imaged by SUBARU/CISCO. The edge-on disk sources are located in the center of the black circles.

2. Observations and data reduction

2.1. VLT/ISAAC imaging

2.1.1. Observations

Near-infrared J [1.11–1.39 μm], H [1.50–1.80 μm], and Ks [2.03–2.30 μm] broad-band images of young stellar sources in southern star forming regions were obtained on 28 April 1999 with the ESO VLT/UT1 (“Antu”) and the facility Infrared Spectrometer And Array Camera (ISAAC, Moorwood et al. 1998). The observations were carried out with the short-wavelength channel of ISAAC, which is equipped with a 1024×1024 Hawaii Rockwell HgCdTe array. The pixel scale was $0\farcs147$ pixel^{-1} and the seeing was $\approx 0\farcs35$ (FWHM) in Ks. Two fields were centered between Elias 29 and WL 19, and between WLY 43 and 44, respectively. Total exposure times were 240s in H and 120s in Ks for the Elias 29/WL 19 field, and 640s in J, 320s in H, and 150s in Ks for the WLY 43/44 field. Fig. 1 illustrates the location of the two ISAAC pointings.

2.1.2. Data reduction and analysis

Two bipolar reflection nebulosities intersected by dark lanes were detected. The objects closely resemble edge-on circumstellar disk sources in Taurus and Orion, and in the following we refer to them as “disk 1” and “disk 2”. A close-up of the two new edge-on disk sources, and a comparison to edge-on disks in Taurus is presented in Fig. 2. Absolute positions were determined using 2MASS data products and relative offsets measured on the ISAAC frames. The photometric calibration is based on the observations of infrared standard stars, and photometric measurements from the 2MASS point source catalog. Coordinates and near-infrared photometry of the disk sources are summarized in Table 1.

2.2. SUBARU/CISCO imaging and spectroscopy

2.2.1. Observations

Long-slit K-band spectra were obtained on 18 June 2000 (“disk 2”) and 16 July 2000 (“disk 1”) with the SUBARU telescope and the Cooled Infrared Spectrograph and Camera for OH suppression (CISCO, Motohara et al. 1998). CISCO is equipped with a 1024×1024 Hawaii Rockwell HgCdTe array and has a pixel scale of $0\farcs111$ pixel^{-1}. The slit-width was $1''$ and the slit was oriented north-south. Individual exposure times were 60s and 100s, yielding a total integration time of 240s and 400s

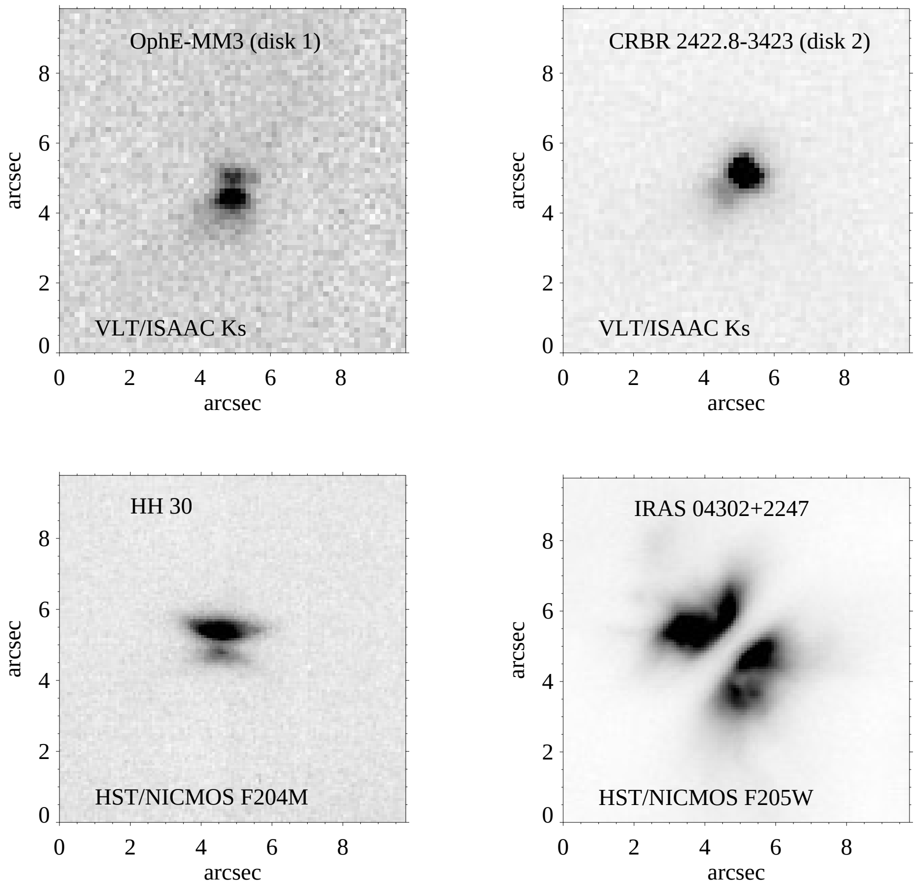

Fig. 2. Edge-on circumstellar disk sources in Ophiuchus and Taurus. In comparison to isolated disks in Taurus, the Ophiuchus disks and their reflection nebulosities are more compact. For the disk sources in the Ophiuchus region, North is up and East is to the left.

for "disk 2" and "disk 1", respectively. Deep dithered K'-band [1.96–2.30 μm] imaging data of disk 1 were obtained on 16 July 2000 (Fig. 3). The seeing on the coadded 800s exposure is $0\farcs4$.

2.2.2. Data reduction and analysis

The data reduction included sky subtraction, and a removal of the geometrical distortion of the 2D spectra. Telluric features were removed by dividing the spectrum of each disk by the spectrum of the standard star. As the observations were obtained under a relatively high airmass of 1.6 to 2.0, the removal of the telluric features was not perfect. The instrumental response was removed by applying an appropriate library spectrum (Pickles 1998). The resulting spectra are shown in Fig. 4. No variation in the spectra across the objects was seen, giving further evidence that the objects are indeed reflection nebulosities.

2.3. ISO observations

The Ophiuchus region has been observed multiple times by ISO (Kessler et al. 1996). The regions including disks 1 and 2 were covered by pointed ISOCAM (Césarsky et al. 1996) observations and by larger scale raster scans with ISOCAM and ISOPHOT (Lemke et al. 1996). HH 30 was also observed by ISOCAM and ISOPHOT (PI: K.R. Stapelfeldt, see Stapelfeldt & Moneti 1999). Basic science data were retrieved from the ISO archive and reprocessed using the latest versions (as of June 2000) of the CIA and PIA software packages.

Disk 2 is detected in several ISOCAM observations towards WLY 2-43 at wavelengths between 4.5 μm and 11.3 μm. Large area raster scans of the regions including disk 1 and disk 2 (Abergel et al. 1996) suffer from memory effects due to brighter sources in the vicinity of the disk sources. It was therefore not possible to derive precise flux values from the large area scans. The ISOCAM fluxes of disk 2 and HH 30 are summarized in Table 2.

ISOPHOT maps at 60 and 100 μm detect and resolve Elias 2-29 and WLY 2-43. Disks 1 and 2, however, are located in the wings of the point spread function of the much brighter sources (FWHM for ISO is 20″ and 35″ at wavelengths of 60 μm and 100 μm, respectively), and were not detected as individual sources.

2.4. HST/NICMOS observations

HST/NICMOS observations of HH 30 were retrieved from the HST archive. The data had been obtained as part of GTO 7228 (PI E. Young). IRAS 04302+2247 was studied by Padgett et al. (1999). The NICMOS data were processed using the standard IRAF/STSDAS data reduction pipeline, and the most current calibration files.

Table 2. ISOCAM fluxes of edge-on disk sources.

Target	4.5 μm [mJy]	6.0 μm [mJy]	6.8 μm [mJy]	7.7 μm [mJy]	9.6 μm [mJy]	11.3 μm [mJy]	12 μm [mJy]	14.3 μm [mJy]
CRBR 2422.8−3423	260±30	400±30	400±40	410±10	150±20	330±30	...	...
HH 30	3.0±0.8	...	2.1±0.8	...	2.3±0.8	...	2.7±0.8	3.9±0.8

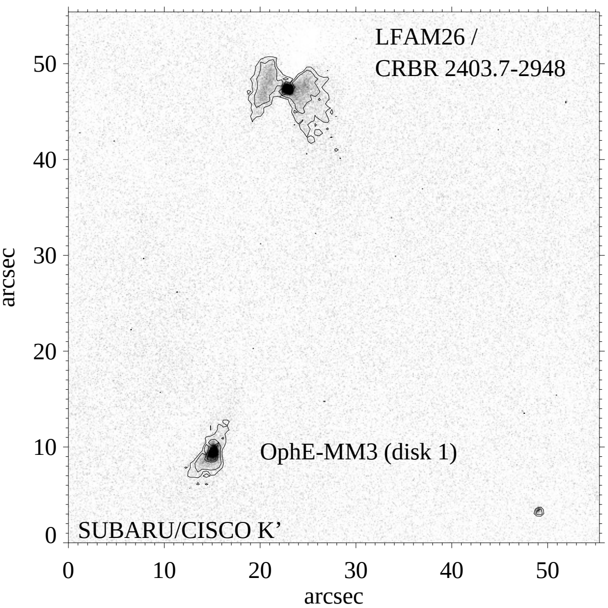

Fig. 3. Deep K' band imaging of disk 1 (OphE-MM3) reveals that the bipolar reflection nebulosity stretches out for ≈5″ above and below the plane of the disk. LFAM 26 (CRBR 2403.7−2948) is associated with a bipolar reflection nebulosity intersected by a central dust lane as well. Unlike disk 1 and 2, however, a central point source is visible. North is up and East is to the left.

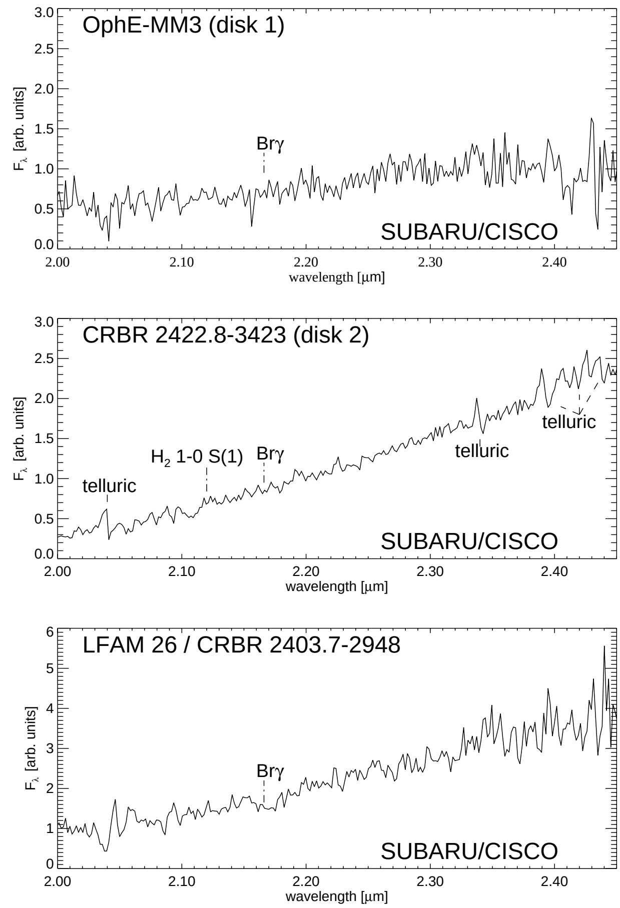

Fig. 4. K-band spectra of disk 1, disk 2, and LFAM26 obtained with SUBARU/CISCO. All three sources exhibit a featureless continuum and show no signs of underlying stellar photospheres, or accretion and outflow signatures (e.g., H_2 or Brγ emission).

3. Discussion

3.1. Disk 1 (OphE-MM3)

The position of disk 1 agrees to within 1″ with the position of the millimeter continuum source OphE-MM3 (Motte et al. 1998). This millimeter source was detected as part of a detailed 1.3mm continuum survey of the Ophiuchus star forming region. Because of the lack of any known counterpart shortward of 1.3 mm, Motte et al. (1998) classify OphE-MM3 as a compact starless core. Motte et al. (1998) note that the millimeter continuum emission of OphE-MM3 is more centrally peaked and does not exhibit any inner flattening as other starless cores in their sample.

The near-infrared counterpart to OphE-MM3 is easily detected on the VLT/ISAAC observations in H and Ks. The high-spatial resolution VLT data reveal that the relative faintness of OphE-MM3 is due to the orientation of its circumstellar disk. The disk is seen close to edge-on, and appears as a central absorption band between the bipolar reflection nebulosity (Fig. 2). The Ks-band peak surface brightness ratio between the southern and the northern half of the reflection nebulosity is 2.1 to 1. OphE-MM3 can also be identified as a 3σ detection on the 2MASS K-band atlas data. Because of its proximity to the K=6$^{\rm m}$8 source Elias 2-29 (10$''$49 south and 48$''$08 east of OphE-MM3), and the increased local background due to diffuse near-infrared emission, however, it must have been overlooked in previous infrared surveys of the ρ Oph region. The deeper SUBARU/CISCO K'-band images of OphE-MM3 reveal that the bipolar reflection nebulosity extends for ≈5″ above and below the plane of the disk (Fig. 3). The K-band spectrum of OphE-MM3 does not show any strong emission lines (Fig. 4).

For young stellar objects, the mass in the disk and the infalling envelope can be derived from 1.3 mm continuum observations (Beckwith et al. 1990). Motte et al. (1998) measure a peak flux beam^{-1} of 60±10 mJy for OphE-MM3. Assuming the standard set of parameters, i.e., T=30 K, $\kappa_{1.3\rm mm}$=0.01 cm^{2}g^{-1}, a gas to dust ratio of $\approx$100, and a distance of 150 pc yields a mass of 0.015 $M_\odot$, i.e., about the same mass typically assumed for the "minimum solar nebula" (e.g., Yorke et al. 1993).

3.2. Disk 2 (CRBR 2422.8−3423)

This source has been detected in previous near-infrared observations (CRBR 2422.8−3423 – Comerón et al. 1993; [SKS95] 162422.8-243422 – Strom et al. 1995; BKLT J162724−244103 – Barsony et al. 1997) and is included in the 2MASS point source catalog. CRBR 2422.8−3423 is located 12$''$.72 south and 31$''$.75 west of WLY 2-43. Similar to OphE-MM3, the VLT/ISAAC observations reveal CRBR 2422.8−3423 as a bipolar nebulosity intersected by a central dust lane. The source is detected on the ISAAC H- and Ks-band frames, but not in the J-band. The magnitudes derived from the VLT/ISAAC and 2MASS data are H=18$^{\rm m}$.0 and Ks=13$^{\rm m}$.3. The Ks-band magnitude is in good agreement to the measurements by Comerón et al. (1993) and Barsony et al. (1997). In Ks, the peak surface brightness ratio between the north-western and the south-eastern halves of the reflection nebulosity is 11 to 1. The larger brightness ratio indicates that the disk plane of CRBR 2422.8−3423 is farther from an edge-on inclination than the disk of OphE-MM3.

CRBR 2422.8−3423 has very red near-infrared colours (Table 1). The steeply rising continuum towards longer wavelengths is also apparent in the K-band spectrum (Fig. 4). No signs of an underlying stellar photosphere or accretion and outflow signatures, like H_2 or Brγ emission lines, are present. There is also no evidence of a CO band at 2.3 μm. The featureless K-band continuum suggests that the observed K-band radiation is largely due to reprocessed photons from hot dust near the star.

Motte et al. (1998) identify CRBR 2422.8−3423 as an unresolved 1.3 mm continuum source with a peak flux beam^{-1} of 40$\pm$10 mJy. This corresponds to a mass of 0.01 $M_\odot$ for the disk and the infalling envelope, again in good agreement with the mass of the "minimum solar nebula".

3.3. LFAM 26 (CRBR 2403.7−2948)

The deep SUBARU/CISCO K'-band imaging reveals another source with a bipolar reflection nebulosity $\approx$40$''$ to the north of disk 1 (Fig. 3). This object has previously been detected at infrared and radio wavelengths (LFAM 26 – Leous et al. 1991; [GY92] 197 – Greene & Young 1992; CRBR 2403.7−2948 – Comerón et al. 1993; [SKS95] 162403.8-242948 – Strom et al. 1995). Motte et al. (1998) measure a peak flux beam^{-1} of 75$\pm$10 mJ at 1.3 mm. The disk/envelope around LFAM 26 thus appears to be the most massive among the three Ophiuchus sources discussed in this letter. The wide dust lane and the fact that a central point source is visible distinguishes this source from the two edge-on disks.

3.4. Comparison to HH 30 and IRAS04302+2247

The two best studied examples for edge-on circumstellar disks are HH 30 (Burrows et al. 1996, Stapelfeldt et al. 1998) and IRAS 04302+2247 (Lucas & Roche 1998, Padgett et al. 1999). With a 1.3 mm continuum flux of 35 mJy (Reipurth et al. 1983), the amount of circumstellar dust in HH 30 is comparable to CRBR 2422.8−3423, and somewhat less than in OphE-MM3. The disk and envelope of IRAS 04302+2247 (F_ν = 150 mJy at 1.1 mm, Hogerheijde et al. 1997) is 3 to 4 times more massive.

The peak surface brightness ratio of the two parts of the bipolar reflection nebulosity of HH 30 in the HST/NICMOS F204M filter is 3.7 to 1, i.e., intermediate between OphE-MM3 and CRBR 2422.8−3423. The inclination angle of the disk of HH 30 with respect to the line of sight as derived by Burrows et al. (1996) is $\leq$10°.

Fig. 2 illustrates the morphology of four edge-on circumstellar disk sources. IRAS 04302+2247 is more extended and appears to be in an earlier evolutionary stage than the 'bare-disk' system HH 30. Similar to HH 30, the disk of OphE-MM3 exhibits a hint of flaring, whereas the central dust lane of CRBR 2422.8−3423 is flat. The extended reflection nebulosities outline the interface between an outflow cavity and the infalling circumstellar envelope (see, e.g., Wilkin & Stahler 1998). Like IRAS 04302+2247, OphE-MM3 and CRBR 2422.8−3423 are more deeply embedded and thus appear to be younger than HH 30, which has already lost most of its envelope material.

Fig. 5 displays the spectral energy distribution (SED) of CRBR 2422.8−3423 and HH 30 for wavelengths between 1 μm and 1.3 mm. While both sources have very similar K band brightness and exhibit about the same 1.3 mm continuum flux, the overall shape of the SED is vastly different. The SED of CRBR 2422.8−3423 is rising steeply in the NIR, peaks at around 5 μm, and is slowly declining towards longer wavelengths. A sharp dip in the SED is apparent at 9.6 μm. The data confirm the classification of CRBR 2422.8−3423 as a Class I source as suggested by Motte et al. (1998). The SED of HH 30 peaks at around 2 μm and shows a shallow and very broad dip around 10 μm.

As a preparation for the ISO and SIRTF missions, Boss & Yorke (1996) carried out extensive radiative hydrodynamical simulations to study the effect of disk geometry and physical parameters like disk mass, stellar mass, dust opacity, or accretion rate on the SED of circumstellar disks.

The inclination of a disk to the line of sight has a strong impact on the overall SED. Close to edge-on, a disk source is almost entirely seen in scattered light out to wavelengths of 20 μm. Edge-on orientation also causes the ice band at 3 μm and the silicate feature at 10 μm to be seen in emisison. Millimeter fluxes are hardly affected by the disk's inclination. For a less edge-on inclination the circumstellar envelope and the outer parts of the disk become optically thin in the mid-infrared, and continuum emission from the warm, inner disk is detected. As a consequence, the silicate feature can be seen in absorption. The simulations by Boss & Yorke (1996) also indicate that the silicate absorption feature becomes more pronounced with increasing disk mass, as a higher disk mass leads to a higher central plane temperature of the inner disk.

The simulations nicely explain the SED of the edge-on disk sources CRBR 2422.8−3423 and HH 30. HH 30 is seen so close

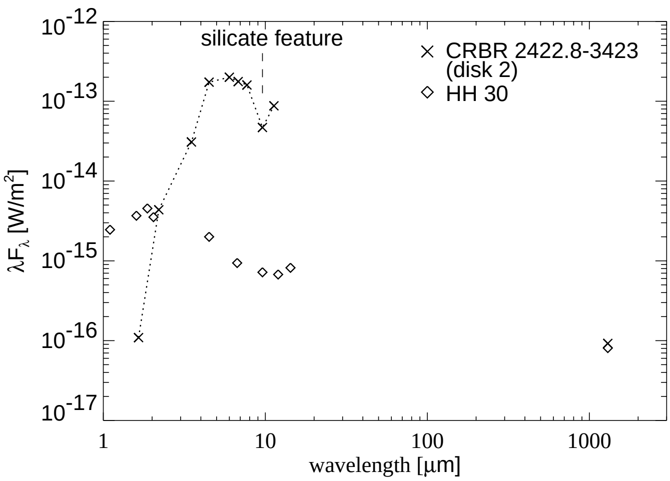

Fig. 5. Spectral energy distribution of CRBR 2422.8−3423 (disk 2) and HH 30. Both sources exhibit about the same flux at 2.2 μm and 1.3 mm. The slightly larger inclination of CRBR 2422.8−3423's disk allows the warm, inner disk to become detectable at NIR to MIR wavelengths. The dip at 9.6 μm can be explained by absorption due to the silicate feature. The spectral energy distribution of HH 30, whose disk is seen closer to edge-on than in the case of CRBR 2422.8−3423, is dominated by scattered light out to wavelengths of 10 μm.

to edge-on that only scattered light is detected out to a wavelength of 10 μm. Both the faintness of HH 30 and the limited spectral resolution of the ISOCAM bands might contribute to a non-detection of a silicate emission feature. The disk of CRBR 2422.8−3423 is oriented less edge-on, and the warm, inner disk can be detected in the mid-infrared. The sharp dip at 9.6 μm in the SED of CRBR 2422.8−3423 is due to silicates seen against the continuum emission from the warm, inner disk.

The observations thus confirm theoretical predictions on the effect of disk geometry and disk inclination on the spectral appearance of a young stellar object.

4. Summary

We have presented the first identification of edge-on circumstellar disks outside of the Orion and Taurus star forming regions. Compared to the majority of edge-on circumstellar disk sources in Taurus, the two edge-on disks in the Ophiuchus region appear to be at an earlier evolutionary stage, as they are still more deeply embedded in their circumstellar envelopes. The high-spatial resolution infrared data confirm that the difference in the spectral energy distribution of CRBR 2422.8−3423 and HH 30 is due to a slight difference in the inclination of the disks to the line of sight, as had been predicted previously by theoretical models.

Acknowledgements. We would like to thank the SUBARU telescope and VLT staff members for their excellent work, and the referee Dr. K.R. Stapelfeldt for his critical and helpful comments. This publication makes use of data products from 2MASS, which is a joint project of UMass and IPAC/Caltech, funded by NASA and NSF. WB acknowledges support by the National Science Foundation and by NASA.

References

Abergel, A., Bernard, J.P., Boulanger, F., Césarsky, C., Désert, F.X. et al. 1996, A&A 315, L329
Barsony, M., Kenyon, S.J., Lada, E.A., Teuben, P.J. 1997, ApJS 112, 109
Beckwith, S.V.W., Sargent, A.I., Chini, R.S., Guesten, R. 1990, AJ, 99, 924
Boss, A.P., Yorke, H.W. 1996, ApJ, 469, 366
Brandner, W., Grebel, E.K., Chu, Y.-H., Dottori, H., Brandl, B., Richling, S., Yorke, H.W., Points, S.D., Zinnecker, H. 2000, AJ 119, 292
Burrows, C.J., Stapelfeldt, K.R., Watson, A.M., Krist, J.E., Ballester, G.E. et al. 1996, ApJ 473, 437
Césarsky, C.J., Abergel, A., Agnèse, P. et al. 1996, A&A 315, L32
Comerón, F., Rieke, G.H., Burrows, A., Rieke, M.J. 1993, ApJ 416, 185
Ghez, A. M., Neugebauer, G., Matthews, K. 1993, AJ 106, 2005
Greene, T.P., Young, E.T. 1992, ApJ 395, 516
Kenyon, S.J., Lada, E.A., Barsony, M. 1998, AJ 115, 252
Kessler, M.F., Steinz, J.A., Anderegg, M.E., Clavel, J., Drechsel, G. et al. 1996, A&A 315, L27
Köhler, R., Leinert, Ch. 1998, A&A 331, 977
Koresko, C.D. 1998, ApJ 507, L145
Leinert, Ch., Zinnecker, H., Weitzel, N., Christou, J., Ridgway, S. T., Jameson, R., Haas, M., Lenzen, R. 1993, A&A 278, 129
Lemke, D., Klaas, U., Abolins, J. et al. 1996, A&A 315, L64
Leous, J.A., Feigelson, E.D., André, P., Montmerle, T. 1991, ApJ 379, 683
Lucas, P.W., Roche, P.F. 1997, MNRAS 286, 895
McCaughrean, M.J., O'Dell, C.R. 1996, AJ, 111, 1977
McCullough, P.R., Fugate, R.Q., Christou, J.C., Ellerbroek, B.L., Higgins, C.H., Spinhirne, J.M., Cleis, R.A., Moroney, J.F. 1995, ApJ 438, 394
Monin, J.-L., Bouvier, J. 2000, A&A 356, L75
Moorwood, A., Cuby, J.-G., Biereichel, P., Brynnel, J., Devillard, N., et al. 1998, The Messenger, 94, 7
Motohara, K., Maihara, T., Iwamuro, F., Oya, S., Imanishi, M., Terada, H., Goto, M., Iwai, J., Tanabe, H., Tsukamoto, H., Sekiguchi, K. 1998, Proc. SPIE, 3354, 659
Motte, F., André, P., Neri, R. 1998, A&A 336, 150
O'Dell, C.R.O., Wen, Z., Hu, X. 1993, ApJ, 410, 686
Padgett, D.L., Brandner, W., Stapelfeldt, K.R., Strom, S.E., Terebey, S., Koerner, D. 1999, AJ 117, 225
Pickles, A.J. 1998, PASP 110, 863
Reipurth, B., Chini, R., Krügel, E., Kreysa, E., Sievers, A. 1993, A&A 273, 221
Sonnhalter, C., Preibisch, T., Yorke, H.W. 1995, A&A 299, 545
Stapelfeldt, K.R., Krist, J.E., Menard, F., Bouvier, J., Padgett, D.L., Burrows, C.J. 1998, ApJ 502, L65
Stapelfeldt, K.R., Moneti, A. 1999, in *The Universe as Seen by ISO*, eds. P. Cox & M.F. Kessler, ESA-SP 427, p. 521
Störzer, H., Hollenbach, D., 1999, ApJ, 515, 669
Strom, K.M., Kepner, J., Strom, S.E. 1995, ApJ 438, 813
Whitney, B.A, Hartmann, L. 1992, ApJ 395, 529
Wilkin, F.P., Stahler, S.W. 1998, ApJ 502, 661
Wilking, B.A, Lada, C.J. 1983, ApJ 274, 698
Yorke, H.W., Bodenheimer, P., Laughlin, G. 1993, A&A 411, 274
Zinnecker, H., Krabbe, A., McCaughrean, M.J., Stanke, T., Stecklum, B., Brandner, W., Padgett, D.L., Stapelfeldt, K.R., Yorke, H.W. 1999, A&A 352, L73